Chemosphere 198 (2018) 139–146

Contents lists available at ScienceDirect

Chemosphere

journal homepage: www.elsevier.com/locate/chemosphere

Humic like substances for the treatment of scarcely soluble pollutants by mild photo-Fenton process

Bruno Caram [a], Sara García-Ballesteros [b], Lucas Santos-Juanes [b, *], Antonio Arques [b], Fernando S. García-Einschlag [a]

[a] Instituto de Investigaciones Fisicoquímicas Teóricas y Aplicadas (INIFTA), CCT-La Plata-CONICET, Universidad Nacional de La Plata, Diag 113 y 64, La Plata, Argentina
[b] Grupo de Procesos de Oxidación Avanzada, Departamento de Ingeniería Textil y Papelera, Campus de Alcoy, Universitat Politècnica de València, E-03801, Alcoy, Spain

HIGHLIGHTS

- waste valorization as the humic-like substances are isolated from urban wastes.
- Use of these substances in waste-water treatment.
- UVA-visible light is used, and hence, it can be driven under real sunlight.
- Extends the use of photo-Fenton towards circumneutral conditions (e.g. avoids acidification).
- Prevents the use of surfactants to dissolve suspensions of non-soluble pollutants.

GRAPHICAL ABSTRACT

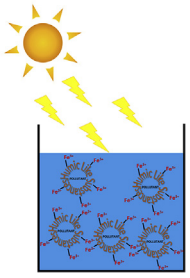

ARTICLE INFO

Article history:
Received 10 September 2017
Received in revised form
13 December 2017
Accepted 15 January 2018

Handling Editor: Jun Huang

Keywords:
Thiabendazole
Photo-Fenton
Humic-like substances
EEM
PARAFAC

ABSTRACT

Humic-like substances (HLS) extracted from urban wastes have been tested as auxiliaries for the photo-Fenton removal of thiabendazole (TBZ) under simulated sunlight. Experimental design methodology based on Doehlert matrices was employed to check the effects of hydrogen peroxide concentration, HLS amount as well as TBZ loading; this last parameter was studied in the range 25–100 mg/L, to include values below and above the limit of solubility at pH = 5. Very satisfactory results were reached when TBZ was above solubility if HLS and H_2O_2 amounts were high. This could be attributed to an interaction of HLS-TBZ that enhances the solubility of the pollutant. Additional evidence supporting the latter interaction was obtained by fluorescence measurements (excitation emission matrices) and parallel factor analysis (PARAFAC).

1. Introduction

The presence of hazardous species in the environment is a serious concern. Compounds such as pesticides or fungicides can easily accumulate in plants, soil or water bodies because of its

* Corresponding author.
E-mail address: lusanju1@txp.upv.es (L. Santos-Juanes).

https://doi.org/10.1016/j.chemosphere.2018.01.074
0045-6535/

resistance to the action of sunlight or microorganisms. Furthermore, the solubility of many of these pollutants is low and they are applied in suspensions or emulsions at concentrations above their solubility limit to ensure its presence in plants or soils during large periods of time (Ibarz et al. (2016)).

Advanced oxidation processes (AOP) have been successfully explored as a procedure to treat low soluble pollutants present in soil by combining a washing step with a later oxidation process (Villa et al. (2010)). One of the most used AOP is the photo-Fenton process, which consists in the use of iron salts to catalyze the decomposition of hydrogen peroxide into highly reactive species, such as hydroxyl radical (Pignatello et al. (2006)). The reaction has an optimum pH, namely 2.8, in order to prevent iron deactivation via formation of hydroxides. Irradiation results in an acceleration of the photocatalytic process and sunlight can be used for this purpose (Malato et al. (2009)). However, this acidic pH is a major drawback for large scale applications or 'in situ' treatments. Hence, research on modified photo-Fenton processes able to work at mild conditions is meaningful (Santos-Juanes et al. (2017)). One of these strategies involves the use of chemical auxiliaries to extend the photocatalytic role of iron salts to a milder pH, by forming photoactive complexes with iron. Carboxylates such as oxalate, EDDS or citric acid have been used for this purpose with satisfactory results, although in most cases these chemicals are consumed in the process (Soares et al. (2015), Huang et al. (2012), Klamerth et al. (2012), De Luca et al. (2014)).

Macromolecules have been employed as chelating agents for photo-Fenton, among them, humic-like substances (HLS). HLS can be obtained from different sources; for instance, soluble bioorganic substances (SBO) are a group of HLS that can be isolated from urban wastes following a procedure described elsewhere (Montoneri et al. (2011a,b)). Some experiments have shown that SBO are able to extend the domain of applicability of photo-Fenton to pH values of ca. 5, with only a slight loss of efficiency which could be considered as acceptable (Gomis et al. (2015a)). Interestingly, recent fluorescence measurements have demonstrated the high ability of SBO to complex iron at an optimum pH of 5 (García Ballesteros et al. (2017)). In addition to this, SBO have been described to have surface active properties (Negueroles et al. (2017)). The surfactant behaviour of SBO would result in a double benefit, as in addition to iron complexation to extend photo-Fenton, they might also enable dissolving scarcely soluble pollutants and a pre-association between the target compound and the catalyst, namely the Fe-SBO complex. Potential applications for this strategy are rinsing of bottles or surfaces exposed to chemicals (Malato et al. (2000)) or soil remediation (Mulligan et al. (2001)). Substances such as organic fungicides might be involved in both scenarios as they commonly show low solubility; when fungicides are applied, only partly reach the crops, while and important amount of them can be found in soils (Reichenberger et al. (2007)). In addition, bottles containing these substances and plastics of greenhouses must be cleaned before disposal, generating a polluted effluent. In this context, there is some information on the use of photo-Fenton for soil washing effluents containing pesticides (Villa et al. (2010)).

With this background, the aim of this work is to investigate the positive role of HLS on photo-Fenton process, as both chelating agent and solubility enhancer, when treating suspensions of pollutants at concentrations beyond their limit of solubility. Thiabendazole (TBZ) has been used as model compound, as it is a widely employed broad-spectrum systemic fungicide used in all kinds of crops, especially fruit and vegetables (Ibarz et al. (2016)). It exhibits moderate-low solubility in the mild acidic pH domain (Cassens et al. (2013)) what enables performing experiments below and above this value. SBO were the type of HLS chosen, as important information on their behaviour in photo-Fenton systems at different pH values is available. Experimental design methodology based on Doehlert matrices has been employed to obtain surface responses, which are useful to study the effect of operational parameters on TBZ degradation.

2. Experimental section

2.1. Reagents

TBZ was supplied by Sigma-Aldrich. Its purity was 99% and it was used as received. $FeCl_3.6H_20$ (Panreac) was used as source of iron. Hydrogen peroxide (30% w/w) was also provided by Panreac. Water employed in all solutions was Milli-Q grade.

The type of SBO employed in this work was CVT230, which was kindly supplied by University of Turin. Home gardening and park trimming residues (GR) piles aerated for 230 days were used as sourcing materials. The procedure as well as the characterization of the product have been previously described in detail (Montoneri et al. (2011a,b)). The SBO isolation was performed in a pilot plant at the Studio Chiono&Associati in Rivarolo Canavese, Italy. It consists in different stages: a) basic digestion of the raw sourcing material, b) elimination of the non-soluble fraction, c) concentration of the macromolecules also by ultrafiltration and d) drying of the retentate. CVT230 contains a 38% of carbon and a 4% of nitrogen, with a 72% of volatile solids. Aliphatic chains represent about twice the aromatic structures, carboxylic acids being the most representative of the functional groups. More details on the physicochemical properties of these substances can be found elsewhere (Gomis et al., 2015b).

2.2. Experimental set-up

Experiments were performed in a cylindrical Pyrex vessel (55 mm i.d.). Irradiations were carried out with a solar simulator (Sun 2000, ABET Technologies) equipped with a 550 W Xenon Short Arc Lamp; a glass filter was employed to cut off the residual radiation below 300 nm. With this configuration, the solar simulator had an irradiance of 75 W/m^2. This value was obtained with an Acadus 85 radiometer with a response range between 290 and 370 nm.

For each experiment, the reactor was loaded with 250 mL of solution containing the SBO (in the range 10–70 mg/L), the pollutant (25–100 mg/L) and iron (5 mg/L). The initial pH was adjusted to the desired value (2.8 or 5.0) by adding diluted sulphuric acid and was left free once the reaction started. The initial concentration of H_2O_2 was in the range 34–510 mg/L. Samples were periodically taken for analysis; they were diluted 1.6:0.3 with methanol to ensure complete dissolution of thiabendazole and to prevent further changes in the composition due to the excess of H_2O_2; then they were filtered through polypropylene (VWR, 0.45 μm).

2.3. Analysis

The concentration of TBZ was monitored by liquid chromatography. A Perkin Elmer model Flexar UPLC FX-10 was employed, equipped with a reverse phase column (Brownlee Analytical DB-C18). The eluent consisted in an isocratic mixture of acetonitrile (5%) and water (95%) at a 0.3 ml/min flow. Detection was based on UV–vis spectrometry at 300 nm.

Samples were also analysed by UV–vis spectroscopy, using a UH5300 spectrometer (Hitachi). Spectra were recorded in the 190–500 nm range. Fluorescence emission-excitation matrices were obtained with a modular fluorimeter QuantaMaster (PTI).

Samples were excited in the range 250–550 nm and emission was recorded in the range 300–600 nm. Before measurements, 2 ml of sample were diluted with 1 ml of methanol and 3 ml of water. pH measurements were performed using a Crison (BASIC 20^+ model) pH-meter.

2.4. Experimental design

To assess the effect of three operational variables (TBZ, SBO and hydrogen peroxide concentrations) an experimental design methodology based on a Doehlert array was used (Ferreira et al. (2004)). A total of 15 experiments (k^2+k+1, where k is the number of analysed variables, 3 in this study, plus two replicates of the central point) were performed. Being the aim of this work determining the effect of SBO in the treatment of non-soluble substances, the range of studied TBZ concentrations should be above and below the limit of solubility for this compound, which was ca. 70–75 mg/L at pH = 5; hence, initial concentrations of 25 mg/L, 62.5 mg/L and 100 mg/L were tested. The concentration of SBO were varied between 10 and 70 mg/L at seven levels. Finally, hydrogen peroxide was tested at five levels in the range 34 mg/L – 510 mg/L; this range was chosen because of the different amounts of oxidizable organics present in the experiments: the upper limit was the stoichiometric amount of hydrogen peroxide required to completely mineralize the highest concentration of TBZ plus an excess of 20%, and the lower limit was the stoichiometric amount required to oxidize the lowest concentration of TBZ minus a 20%. The initial pH was in all cases 5. Experimental conditions of all experiments can be found in Table 1.

The irradiation time required to decrease TBZ to 50% of its initial concentration ($t_{50\%}$), obtained from the plot of the relative TBZ concentration vs. time, or the absolute initial TBZ degradation rate (calculated from the initial slope of TBZ profile against time) were used as responses. The software Statgraphics Centurion XVI was used for response surface model fitting by means of the least squares method.

2.5. Analysis of fluorescence datasets

Parallel factor analysis (PARAFAC) (Andersen and Bro (2003)) was used to decompose the sets of Excitation-Emission-Matrices (EEMs) into independent factors (García-Ballesteros et al. (2017), Su et al. (2015)). Briefly, given a 3-way array structure containing the EEMs of several samples (**X**), the PARAFAC algorithm decomposes **X** into three matrices that contain the relative contribution profiles (A), the normalized emission spectra (B) and the normalized excitation spectra (C), for each of the factors that compose the observed fluorescent signals. Pre-processing steps, including the correction of inner-filter effects (i.e., primary and secondary), blank subtraction and the removal of scattering signals (i.e., Rayleigh and Raman), were followed (Ohno (2002), Bahram et al. (2006)). PARAFAC models from two to six factors were tested. In all cases, non-negativity and unimodality constraints were used to obtain chemically relevant results. The correct number of factors was assessed by the analysis of the physical sense of spectral loadings as well as the evaluation of the distribution of residuals.

Table 1
Experimental points used to obtain the response surface (Doehlert matrix). The concentrations of H_2O_2, TBZ and SBO are expressed as mg/L^{-1}. Data given in the last two columns correspond to a) the time (in min) required to decrease concentration of each EP to 50% of the initial value, and b) the initial reaction rate for the same reaction.

Coded values			Uncoded Values			Responses	
X_1	X_2	X_3	$[H_2O_2]$ (mg/L)	[SBO] (mg/L)	[TBZ] (mg/L)	$t_{50\%}$ (min)	r_{Ini} (mg/(L·min))
0	0	0	272	40	62.5	37	0.863
1	0	0	510	40	62.5	28	1.225
0.5	0.866	0	391	70	62.5	21	1.644
0.5	0.289	0.817	391	50	100	22	2.300
−1	0	0	34	40	62.5	76	0.375
−0.5	−0.866	0.000	153	10	62.5	56	0.538
−0.5	−0.289	−0.817	153	30	25	24	0.370
0.5	−0.866	0.000	391	10	62.5	44	0.581
0.5	−0.289	−0.817	391	30	25	19	0.673
−0.5	0.866	0	153	70	62.5	32	0.925
0	0.577	−0.817	272	60	25	16	0.833
−0.5	0.289	0.817	153	50	100	32	1.600
0	−0.577	0.817	272	20	100	37	0.600
0	0	0	272	40	62.5	26	1.094
0	0	0	272	40	62.5	31	0.956

3. Results and discussion

3.1. Mild photo-Fenton to remove TBZ in the presence of SBO

A first series of experiments was performed to determine if the presence of SBO was able to improve the ability of photo-Fenton to remove TBZ. The following experiments were carried out: a) Fe(III) + H_2O_2 at pH = 5 under dark conditions, b) irradiation of TBZ + H_2O_2 at pH = 5, c) photo-Fenton at pH = 5 without SBO, d) photo-Fenton at pH = 5 with SBO, e) photo-Fenton at pH = 2.8 without SBO, f) photo-Fenton at pH = 2.8 with SBO. The concentration of TBZ was 62.5 mg/L which is a value close to its solubility limit at pH 5 (i.e., 75 mg/L); iron concentration was 5 mg/L and, when present, the SBO concentration was 40 mg/L and the initial amount of hydrogen peroxide was the stoichiometric amount required to mineralize TBZ, namely 272 mg/L. Kinetic profiles can be found in Fig. 1; photo-Fenton at pH = 2.8 was always faster than that at pH = 5; this is not a surprising result, as 2.8 is the optimum pH for photo-Fenton. In fact, at pH = 5 only photo-Fenton in the presence of SBO could achieve a complete TBZ removal; this agrees with previous results, which shown that SBO enhanced photo-Fenton at circumneutral pH by avoiding, via iron complexation, catalyst inactivation (Gomis et al. (2014)). In the same work, it was reported that SBO may play a detrimental role at pH = 2.8, most probably due to a competition between SBO and pollutant for the reactive species. However, in experiments here reported, the effect of SBO was positive even in acidic media: this cannot be attributed

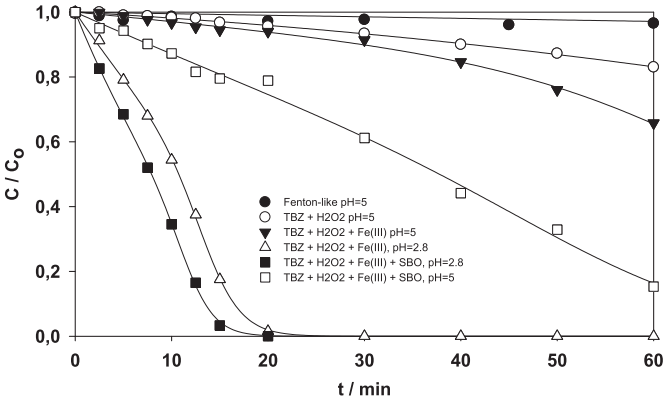

Fig. 1. Plot of the relative concentration of TBZ vs irradiation time under the following experimental conditions $[TBZ]_0 = 62.5$ mg/L, $[H_2O_2] = 272$ mg/L, when was present, [Fe(III)] = 5 mg/L and [SBO] = 40 mg/, (●) dark Fenton at pH = 5, (○) TBZ + H_2O_2 at pH = 5, (Δ) photo-Fenton at pH = 2.8, (■) photo-Fenton with SBO at pH = 2.8, (▼) photo-Fenton at pH = 5, (□) photo-Fenton with SBO at pH = 5.

to iron complexation (this is not required at this pH to prevent iron inactivation) and suggests that the surfactant role of these macromolecules might result in a pre-association of TBZ with the SBO/Fe system, thus favouring the reaction between the short-lived reactive species and the pollutant. This effect should be more predominating at higher pollutant concentration, as the competition of SBO for the active species is not so relevant.

In order to gain further insight into the role of SBO in photo-Fenton at pH = 5 and different TBZ initial amounts, a [TBZ] = 62.5 mg/L was chosen for the central point of the experimental design because, as stated above, it is close to the solubility limit of this compound. The lowest and the highest TBZ loadings were 25 and 100 mg/L, with TBZ being completely and partially soluble, respectively. Both the time required to decrease TBZ to 50% of its initial value ($t_{50\%}$) and the absolute initial degradation rate (r_{Init}) were used as response parameters.

It is important to mention that some decrease from the initial pH value of 5 was observed, since values slightly below 4 were recorded at the end of the process. This is a very well-known behaviour due to the release of carboxylic intermediates. However, this change was slow enough to have negligible effect on the kinetics at the early stages of the reaction.

Despite the experimental problems associated with the use TBZ loadings above the solubility limit, the regression coefficient was reasonable (91.4%). Pareto chart (see supplementary material, FS1), show that concentration of hydrogen peroxide and SBO were the most significant parameters. The response surface describing $t_{50\%}$ values is given by Equation (1)

$$t_{50\%} = 37.7 - 0.24\cdot[H_2O_2] - 0.21\cdot[SBO] + 1.34\cdot[TBZ] + 0.00034\cdot[H_2O_2]^2 + 0.00007\cdot[H_2O_2]\cdot[SBO] - 0.00030\cdot[H_2O_2]\cdot[TBZ] + 0.0024\cdot[SBO]^2 - 0.0056\cdot[SBO]\cdot[TBZ] - 0.0071\cdot[TBZ]^2 \quad (1)$$

Despite valuable information can be extracted from the analysis of coefficients of Equation (1), it is difficult to visualize the effect of each parameter in the three-dimensional domain described by this response surface. For this reason, different bi-dimensional functions were obtained by fixing one parameter at a given value since they can be represented by contour plots. Fig. 2 shows plots obtained by using the coefficients of Equation (1) and fixing each parameter at three levels: high, central and low value.

Plots obtained when fixing [SBO] at high, low and central levels (65, 40 and 15 mg/L respectively) followed similar patterns: the $t_{50\%}$ value was mostly ruled by the concentration of peroxide below 150–250 mg/L. Above this point, $t_{50\%}$ became nearly independent of H_2O_2, although a certain loss of efficiency can be appreciated at the highest oxidant concentrations; the detrimental effect of an excess of H_2O_2 has been reported elsewhere and it is attributable to scavenging of the reactive species, namely $OH (Santos-Juanes et al. (2011)). Finally, it can be observed that TBZ loading has only a minor

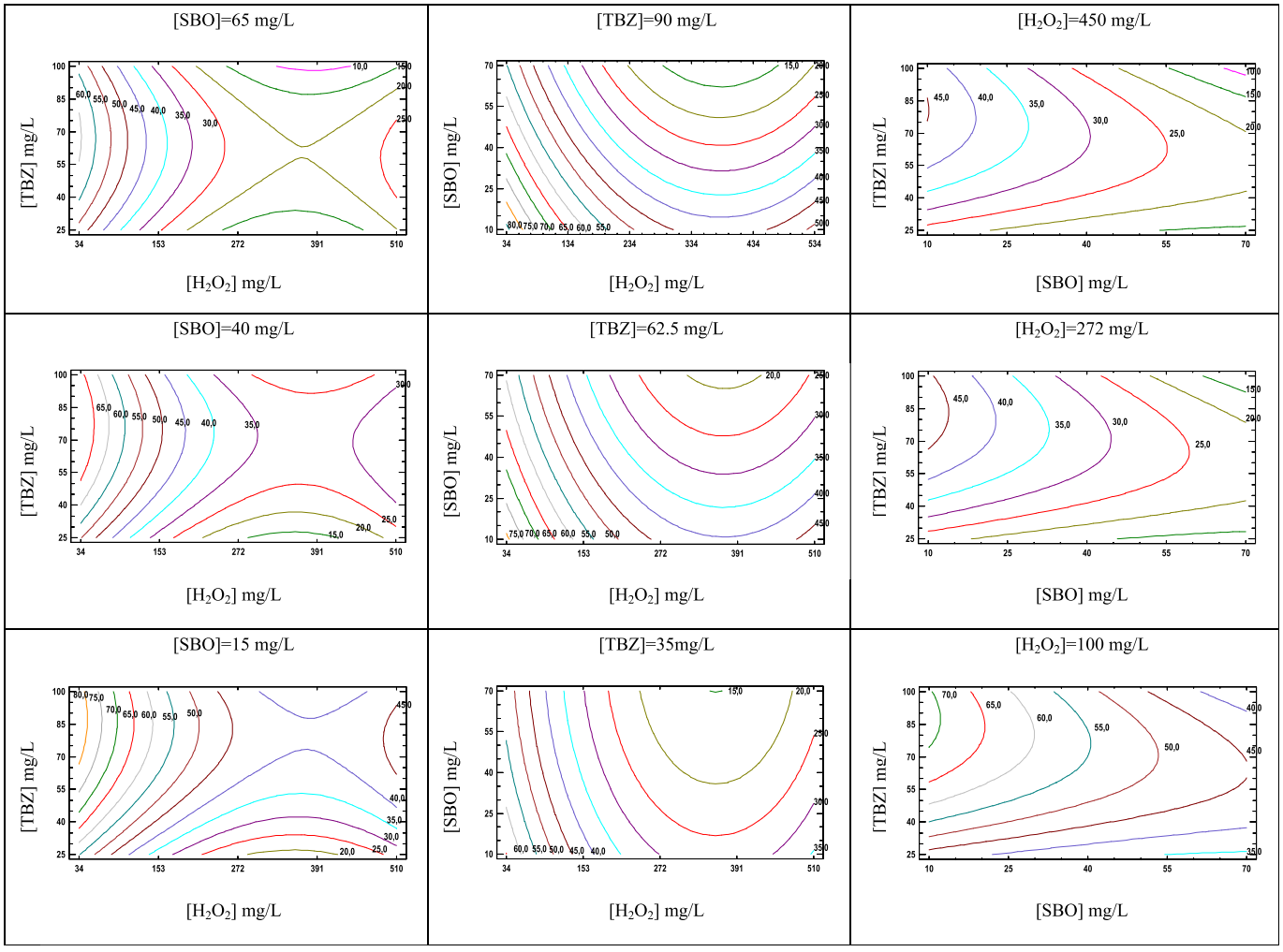

Fig. 2. Contour plots for $t_{50\%}$ values obtained from Equation (1) at selected values of each studied parameter.

effect at high concentrations of SBO, while for low amounts of added SBO, an increase in TBZ loading results in a higher $t_{50\%}$, and hence, a loss of efficiency. This seems a first hint that SBO plays a favourable role by enhancing TBZ solubility.

The initial loading of TBZ was also fixed at three points (90, 62.5, and 35 mg/L). The effect of H_2O_2 was also clear in this case, with optimal values in the range 300–400 mg/L. However, very important differences in the plots can be appreciated regarding to the effect of SBO concentration. For the lowest TBZ amount, the contour lines are predominantly vertical, showing that the effect of $[H_2O_2]$ is much more important than that of [SBO]; however, as TBZ loading approaches to the solubility limit, contour lines become more oblique, showing an increase of the importance of the [SBO]; this agrees with this macromolecule playing a surfactant role, hence favouring the contact between the reactive species and the pollutant.

The same procedure was followed with the concentration of hydrogen peroxide. Very similar values of $t_{50\%}$ were obtained at the central and high levels (272 and 450 mg/L) while treatment efficiencies significantly decrease at the lowest level (100 mg/L), indicating that a certain amount of hydrogen peroxide is required for achieving important conversion degrees within the first hour of treatment. Interestingly, in all three scenarios the worst performance was reached at high pollutant loadings and low [SBO], indicating that close or above TBZ solubility the presence of SBO is required for an efficient treatment, in agreement with previous observations.

A response surface was also obtained (equation (2)) from the absolute initial reaction rates (r_{init}, given as mg converted per minute and litter) of TBZ removal (data shown in Table 1). The regression coefficient was also good (93.7%) and Pareto chart (see supplementary material, FS1) shows that in this case all three parameters became significant, as well as the interaction between the concentrations of SBO and TBZ. Data based on r_{init} can provide complementary information to $t_{50\%}$, as the time required to decrease the initial concentration in a 50% is a relative value that characterizes the overall transformation rate while the initial rate is an absolute parameter describing the system behaviour at the beginning of the treatment.

$$r_{init}\ (mg\ L^{-1}\cdot min^{-1}) = 1.13 + 0.967\cdot10^{-3}\cdot[H_2O_2] - 27.4\cdot10^{-3}\cdot[SBO] - 21.7\cdot10^{-3}\cdot[TBZ] - 3.02\cdot10^{-6}\cdot[H_2O_2]^2 + 47.3\cdot10^{-6}\cdot[H_2O_2]\cdot[SBO] - 9.62\cdot10^{-6}\cdot[H_2O_2]\cdot[TBZ] - 6.94\cdot10^{-6}\cdot[SBO]^2 + 0.498\cdot10^{-3}\cdot[SBO]\cdot[TBZ] + 0.086\cdot10^{-3}\cdot[TBZ]^2 \quad (2)$$

As done with $t_{50\%}$, contour plots were obtained by fixing each parameter at three different levels (Fig. 3). When fixing [SBO], it can be appreciated that at the highest level, the r_{init} increases with the amount of TBZ if there is enough availability of hydrogen peroxide. In fact, the plot shows values ranging from below 0.3 mg/(L·min) to

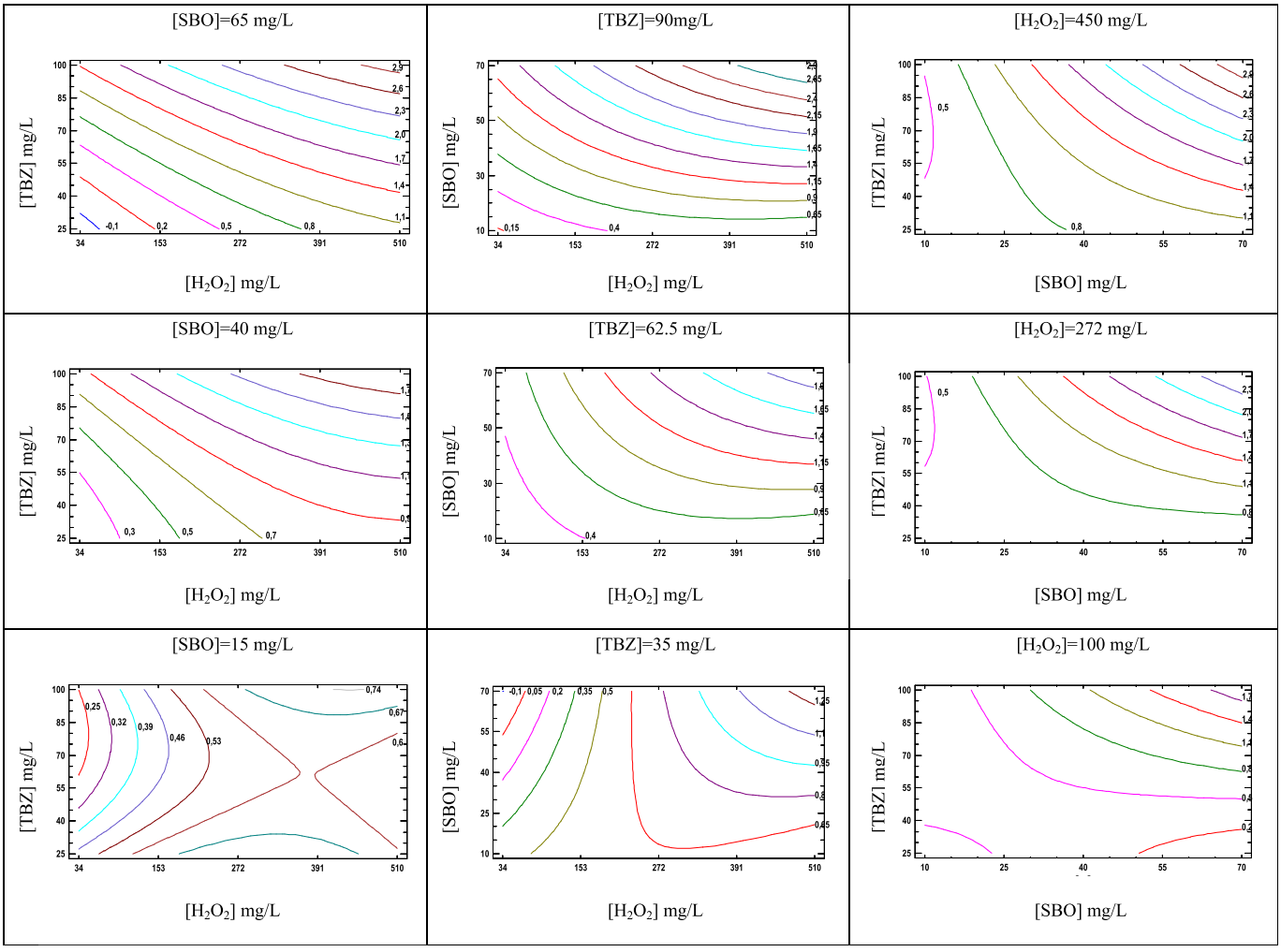

Fig. 3. Contour plots for r_{Init} values obtained from Equation (2) at selected values of each studied parameter.

above 3 mg/(L·min). The same behaviour is observed at the central [SBO] although variation in r_{init} is not so remarkable (values in the range 0.3–1.8 mg/(L·min)). On the contrary, for the low [SBO] no significant variation of r_{init} in the experimental region was observed. When fixing TBZ loading at the highest level, a clear positive effect of SBO can be appreciated, as reaction rate increases with the concentration of this macromolecule; this effect is observed to a minor extent at the central TBZ value and it is practically not found for TBZ fixed at the lowest loading, clearly below the solubility of this compound. Finally, when fixing hydrogen peroxide at the three levels, a strong interaction between the amounts of TBZ and SBO was observed in all cases, as the reaction was faster in the region where the levels of both, SBO and TBZ, were high.

Putting all results together, it can be stated that SBO has a positive role on the decomposition of TBZ when the loading of this pollutant is close or above its limit of solubility, while it is not so evident at lower amounts of TBZ; this is more clearly appreciated when analysing r_{init} than $t_{50\%}$. Furthermore, it can be appreciated that, for high TBZ loadings, increasing [SBO] results in an enhancement of the reaction rates. This is a different behaviour from that reported for other pollutants (pesticides and pharmaceuticals) at concentrations of 5 mg/L (Gomis et al. (2015a,b)), where an optimal SBO concentration was observed and beyond this point, further addition of this substance was detrimental. This was attributed to competition of SBO with the pollutant for the reactive species and the inner filter effect exerted by this coloured substance, which became more important than the enhancement in

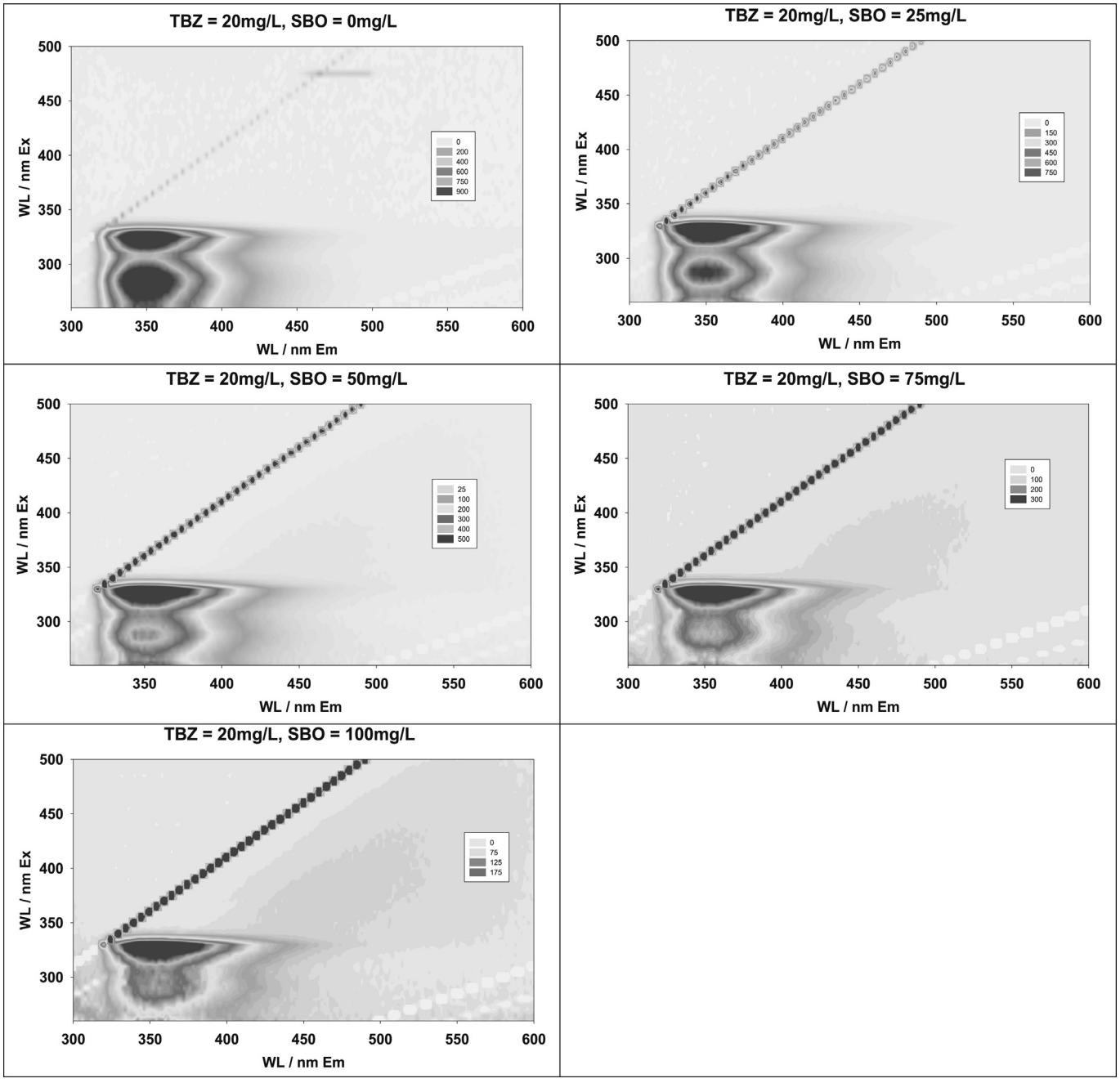

Fig. 4. Absorbance corrected EEM obtained for TBZ solutions in the presence of increasing SBO concentrations.

reactive species generation associated with the iron-complexing ability of SBO. However, when pollutants are close to their solubility limit, an extra factor must be considered, namely the ability of SBO to act as surfactant, which favours the contact between the reactive species and TBZ in solution.

3.2. Mechanistic studies

As the positive role of SBO in the degradation of TBZ in photo-Fenton systems should be attributed to a kind of interaction between the pollutant and the humic-like substance, devoting further research to investigate of the nature of this interaction seems interesting. Since UV–vis spectra did not provide clear evidence of TBZ-SBO interaction, fluorescence measurements were performed. The excitation-emission matrices (EEM) were recorded in solutions containing 20 mg/L of TBZ at increasing concentrations of SBO (0, 25, 50, 75 and 100 mg/L) at pH = 5. EEM are bi-dimensional plots showing the emission of fluorescence at a given wavelength upon excitation at another wavelength (García Ballesteros et al. (2017), Ohno (2002), Bahram et al. (2006), Ohno et al. (2008)); the obtained EEM can be observed in Fig. 4.

In order to gain further insight into the composition of the system under the studied conditions, a PARAFAC analysis was performed. This is a mathematical procedure commonly employed to study complex mixtures, which allows determining the number of fluorescent contributions as well as their spectral features. In this case, the aim of this analysis was to obtain valuable information that supported the interaction between the SBO and the model pollutant. PARAFAC analysis of EEMs shown in Fig. 5 indicated that the experimental data could be adequately fitted to a model consisting in 5 components, the emission and excitation spectra of which can be seen in Fig. 5. Two of these components, with emission maxima at 344 nm and 350 nm, were also observed for TBZ solutions free of BOS and may be ascribed to the acidic (F1) and neutral (F3) forms of TBZ, respectively. Other two factors (whose emission maxima are at 444 and 532 nm) could be assigned to SBO (F4 and F5), according to previous studies performed with these substances (García Ballesteros et al. (2017)). Interestingly, a fifth factor (F2) was found, whose emission maximum was close to 360 nm; this component can solely be observed for solutions where both TBZ and SBO were present, and hence it should be assigned to an interaction TBZ-SBO. Noteworthy, the contribution of this latter factor increases with increasing [SBO].

Additional tests were performed to characterize the fluorescent behaviour of acid and neutral forms of TBZ. In this context, EEM were recorded for TBZ solutions of different pH in the absence of SBO (Fig. SF3, Supporting Information). PARAFAC analysis yielded two main factors, corresponding to acidic and neutral forms of TBZ. Interestingly, a third contribution appeared and it was observed to increase at pH above 4.5. This value is close to the pK_a of TBZ (4.8 according to the literature (Cassens et al., 2013)), in coincidence with the predominance of neutral form of TBZ, which is less soluble than the corresponding acidic form. Furthermore, the first order Rayleigh dispersion band increased, which is commonly observed in the presence of suspended material in the sample (Ohno et al. (2008)). Hence, this third contribution could be associated with the formation of aggregates of the neutral form of TBZ, due to its hydrophobicity. It is important to remark that in the presence of SBO and at pH = 5, the EEM analysed showed no evidence of aggregates, thus providing an additional piece of evidence of the interaction TBZ-SBO, which prevents precipitation of the pesticide.

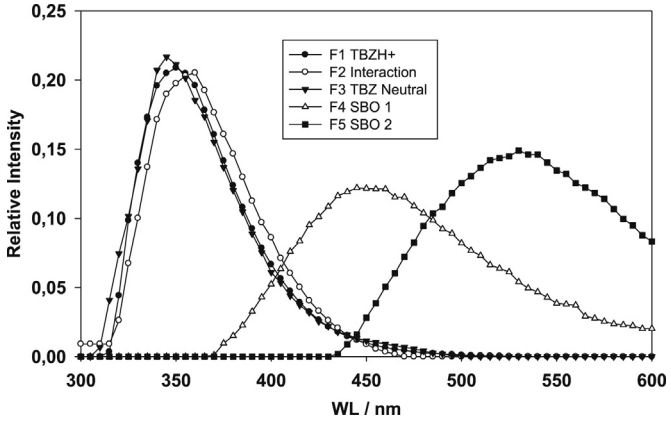

Fig. 5. Emission spectra obtained by PARAFAC decomposition of EEM datasets recorded for TBZ aqueous solution containing different concentrations of SBO.

4. Conclusions

Humic-like substances have been demonstrated as interesting additives for the removal of scarcely soluble pollutants, close or above their limits of solubility, via photo-Fenton processes. This result is interesting in view of applying a procedure that involves combination of soil washing with the SBO, followed by a solar photo-Fenton to treat the obtained effluent. Hence, further research in this field is meaningful, namely with simulated or real soils polluted with the pesticide.

Photophysical studies, based on the analysis of EEM-datasets by the PARAFAC algorithm, have shown the existence of an interaction between the SBO and the model pollutant. This methodology has appeared as especially interesting to unveil mechanistic aspects of photo-oxidative processes when dealing with complex mixtures.

Acknowledgments

Authors want to acknowledge the financial support of Spanish Ministerio de Economía y Competitividad (CTQ2015-69832-C04) and European Union (645551-RISE-2014, MAT4TREAT). The present work was partially supported by UNLP (11/X679), ANPCyT (PICT-2015-0374A) and CONICET (PIP: 12-2013-01-00236CO). B. Caram thank the CONICET for his research graduate grant. F. S. García Einschlag is a research member of CONICET.

Appendix A. Supplementary data

Supplementary data related to this article can be found at https://doi.org/10.1016/j.chemosphere.2018.01.074.

References

Andersen, C.M., Bro, R., 2003. Practical aspects of PARAFAC modeling of fluorescence excitation-emission data. J. Chemometr. 17, 200–215.
Bahram, M., Bro, R., Stedmon, C., Afkhami, A., 2006. Handling of Rayleigh and Raman scatter for PARAFAC modeling of fluorescence data using interpolation. J. Chemometr. 20 (3–4), 99–105.
Cassens, J., Prudic, A., Ruether, F., Sadowski, G., 2013. Solubility of pharmaceuticals and their salts as a function of pH. Ind. Eng. Chem. Res. 52, 2721–2731.
De Luca, A., Dantas, R.F., Esplugas, S., 2014. Assessment of iron chelates efficiency for photo-Fenton at neutral pH. Water Res. 61, 232–242.
Ferreira, S.L.C., dos Santos, W.N.L., Quintella, C.M., Neto, B.B., Bosque-Sendra, J.M., 2004. Doehlert matrix: a chemometric tool for analytical chemistry-review. Talanta 63, 1061–1067.
García Ballesteros, S., Constante, M., Vicente, R., Mora, M., Amat, A.M., Arques, A., Carlos, L., García Einschlag, F.S., 2017. Humic-like substances from urban waste as auxiliaries for photo-Fenton treatment: a fluorescence EEM-PARAFAC study. Photochem. Photobiol. Sci. 16, 38–45.
Gomis, J., Bianco Prevot, A., Montoneri, E., González, M.C., Amat, A.M., Mártire, D.O., Arques, A., Carlos, L., 2014. Waste sourced bio-based substances for solar-driven wastewater remediation: photodegradation of emerging pollutants. Chem. Eng.

J. 235, 236–243.
Gomis, J., Carlos, L., Bianco Prevot, A., Teixeira, A.C.S.C., Mora, M., Amat, A.M., Vicente, R., Arques, A., 2015b. Bio-based substances from urban waste as auxiliaries for solar photo-Fenton treatment under mild conditions: optimization of operational variables. Catal. Today 240, 39–45.
Gomis, J., Gonçalves, M.G., Vercher, R.F., Sabater, C., Castillo, M.A., Bianco Prevot, A., Amat, A.M., Arques, A., 2015a. Determination of photostability, biocompatibility and efficiency as photo-Fenton auxiliaries of three different types of soluble bio-based substances (SBO). Catal. Today 252, 177–183.
Huang, W., Brigante, M., Wu, F., Hanna, K., Mailhot, G., 2012. Development of a new homogenous photo-Fenton process using Fe(III)-EDDS complexes. J. Photochem. Photobiol. Chem. 239, 17–23.
Ibarz, R., Garvín, A., Aguilar, K., Ibarz, A., 2016. Kinetic study and modelling of the UV photo-degradation of thiabendazole. Food Res. Int. 81, 133–140.
Klamerth, N., Malato, S., Aguera, A., Fernandez-Alba, A., Mailhot, G., 2012. Treatment of municipal wastewater treatment plant effluents with modified photo-fenton as a tertiary treatment for the degradation of micro pollutants and disinfection. Environ. Sci. Technol. 46 (5), 2885–2892.
Malato, S., Blanco, J., Richter, C., Maldonado, M.I., 2000. Optimization of pre-industrial solar photocatalytic mineralization of commercial pesticides: application to pesticide container recycling. Appl. Catal. B Environ. 25, 31–38.
Malato, S., Fernández-Ibáñez, P., Maldonado, M.I., Blanco, J., Gernjak, W., 2009. Decontamination and disinfection of water by solar photocatalysis: recent overview and trends. Catal. Today 147, 1–59.
Montoneri, E., Boffa, V., Savarino, P., Perrone, D.G., Ghezzo, M., Montoneri, C., Mendichi, M., 2011a. Acid soluble bio-organic substances isolated from urban bio-waste. Chemical composition and properties of products. Waste Manag. 31, 10–17.
Montoneri, E., Mainero, D., Boffa, V., Perrone, D.G., Montoneri, C., 2011b. Biochemenergy: a project to turn an urban wastes treatment plant into biorefinery for the production of energy, chemicals and consumer's products with friendly environmental impact. Int. J. Global Environ. Issues 11, 170–196.
Mulligan, C.N., Yong, R.N., Gibbs, B.F., 2001. Surfactant-enhanced remediation of contaminated soil: a review. Eng. Geol. 60, 371–380.
Negueroles, P.G., Bou-Belda, E., Santos-Juanes, L., Amat, A., Arques, A., Vercher, R.F., Monllor, P., Vicente, R., 2017. Treatment and reuse of textile wastewaters by mild solar photo-Fenton in the presence of humic-like substances. Environ. Sci. Pollut. Res. 24, 12664–12672.
Ohno, T., 2002. Fluorescence inner-filtering correction for determining the humification index of dissolved organic matter. Environ. Sci. Technol. 36, 742–746.
Ohno, T., Amirbahman, A., Bro, B., 2008. Parallel factor analysis of excitation–emission matrix fluorescence spectra of water soluble soil organic matter as basis for the determination of conditional metal binding parameters. Environ. Sci. Technol. 42, 186–192.
Pignatello, J.J., Oliveros, E., MacKay, A., 2006. Advanced oxidation processes for organic contaminant destruction based on the Fenton reaction and related chemistry. Crit. Rev. Environ. Sci. Technol. 36, 1–84.
Reichenberger, S., Bach, M., Skitschak, A., Frede, H.G., 2007. Mitigation strategies to reduce pesticide inputs into ground- and surface water and their effectiveness; A review. Sci. Total Environ. 384, 1–35.
Santos-Juanes, L., Sánchez, J.L.G., López, J.L.C., Oller, I., Malato, S., Sánchez Pérez, J.A., 2011. Dissolved oxygen concentration: a key parameter in monitoring the photo-Fenton process. Appl. Catal. B Environ. 104, 316–323.
Santos-Juanes, L., Amat, A.M., Arques, A., 2017. Strategies to drive photo-fenton process at mild conditions for the removal of xenobiotics from aqueous systems. Curr. Org. Chem. 21, 1074–1083.
Soares, P.A., Batalha, M., Souza, S.M.A.G.U., Boaventura, R.A.R., Vilar, V.J.P., 2015. Enhancement of a solar photo-Fenton reaction with ferric-organic ligands for the treatment of acrylic-textile dyeing wastewater. J. Environ. Manag. 152, 120–131.
Su, Y., Chen, F., Liu, Z., 2015. Comparison of optical properties of chromophoric dissolved organic matter (CDOM) in alpine lakes above or below the tree line: insights into sources of DOM. Photochem. Photobiol. Sci. 14, 1047–1062.
Villa, R.D., Trovó, A.G., Nogueira, R.F.P., 2010. Soil remediation using a coupled process: soil washing with surfactant followed by photo-Fenton oxidation. J. Hazard Mater. 174, 770–775.